# Identification of Diagnostic Metabolic Signatures in Thyroid Tumors using Mass Spectrometry Imaging

Xinxin Mao [#] , Luojiao Huang [#] , Tiegang Li , Abliz Zeper , Jiuming He [*] , Jie Chen [*,#]

Posted Date: 15 June 2023

doi: 10.20944/preprints202306.1101.v1

Keywords: thyroid follicular adenoma; thyroid follicular carcinoma; mass spectrometry; tumor; diagnose; marker

*Article*

# Identification of Diagnostic Metabolic Signatures in Thyroid Tumors Using Mass Spectrometry Imaging

**Xinxin Mao [1,♯], Luojiao Huang [2,♯], Tiegang Li [2], Zeper Abliz [2], Jiuming He [2,*] and Jie Chen [1,*,♯]**

[1] Department of Pathology, Peking Union Medical College Hospital, Chinese Academy of Medical Sciences and Peking Union Medical College, Beijing 100730, China
[2] State Key Laboratory of Bioactive Substance and Function of Natural Medicines, Institute of Materia Medica, Chinese Academy of Medical Sciences and Peking Union Medical College, Beijing 100050, China
* Correspondence: hejiuming@imm.ac.cn; Jie Chen; email: chenjie@pumch.cn
♯ These authors contributed equally to this work.

**Abstract:** "Gray zone" category tumors in thyroid follicular tumors are difficult to diagnose, especially to distinguish between follicular thyroid adenoma (FTA) and follicular thyroid carcinoma (FTC). This study aimed to assess the diagnostic performance of metabolite enzymes using imaging mass spectrometry to distinguish FTA from FTC and determine the association between metabolite enzyme expression with thyroid follicular borderline tumor diagnosis. Air flow-assisted desorption electrospray ionization mass spectrometry imaging (AFAIDESI-MSI) was used to develop a classification model for the characteristics of thyroid follicular tumors among 24 samples. We analyzed the expression of metabolic enzyme markers in an independent validation set of 133 cases and evaluated the potential biological behavior of 19 borderline thyroid lesions. Phospholipids and fatty acids (FAs) were more abundant in FTA than in FTC ($P<0.001$). The metabolic enzyme panel—including FA synthase and $Ca^{2+}$-independent PLA2, which are closely associated with altered metabolic pathways—was further identified in follicular thyroid tumors. The marker combination showed optimal performance in the validation group (area under the receiver operating characteristic curve, sensitivity, and specificity: 73.6%, 82.1%, 60.6%, respectively). The diagnostic strategy suggested considering a putative role of AFAIDESI-MSI in routine clinical triage for strict follow-up, with low metabolic enzyme expression combined with diagnostic in patients with a thyroid follicular borderline tumor diagnosis.

**Keywords:** thyroid follicular adenoma; thyroid follicular carcinoma; mass spectrometry; tumor; diagnose; marker

## 1. Introduction

Thyroid tumors are the most common endocrine lesions worldwide, and their incidence has continuously increased over the last three decades [1,2] Thyroid tumors arising from follicular cells can generally be categorized into malignant and benign tumors according to their pathology. However, it is sometimes extremely difficult to differentiate thyroid follicular adenoma (FTA) from thyroid follicular carcinoma (FTC). Pathomorphology is used to describe the characteristics of malignant tumors named "atypia," which does not appear in benign tumors. However, this morphological standard does not apply to thyroid follicular neoplasms. FTA cells can show atypia; conversely, the atypia of FTC cells may be gentle or absent, distant metastasis of FTC sometimes occurs, such as in bones or lungs, and the morphology of metastatic tumors is still very mild, similar to that of FTA. Currently, the diagnosis of FTC is defined by capsular and/or vascular invasion; however, this standard is difficult to achieve in frozen sections or even in surgically excised lesions.

Therefore, in the most recent version of the World Health Organization (WHO) classification, certain borderline lesions, including non-invasive follicular thyroid neoplasms with papillary-like nuclear features (NIFTP) and thyroid tumors of uncertain malignant potential (UMP), have been

 doi:10.20944/preprints202306.1101.v1



proposed to classify follicular thyroid neoplasms with questionable capsular or vascular invasion. Given that malignant tumors require more surgical intervention than benign tumors, managing these "gray zone category" follicular tumors remains controversial; thus, the proper classification of thyroid follicular diseases has become an urgent clinical need.

Mass spectrometry imaging (MSI) is a powerful method employed in tumor research, allowing for different molecular species of complex proteins, lipids, and their metabolites to be imaged. The major benefit of MSI is the ability to combine molecular and morphological information. Molecular images generated using mass spectrometry are spatially resolved and correlated with their respective histological images; thus, molecular profiles can be highly tissue-specific and closely related to clinical information. Furthermore, metabolomic research is closely related to the occurrence and development of tumors, and changes in the expression of metabolite molecules and related metabolic pathways are important characteristics of tumor cells. Moreover, metabolomic research based on MSI is a high-throughput approach that can identify molecular information closely related to the occurrence and development of tumors.

The airflow-assisted desorption electrospray ionization (AFADESI)-MSI method under ambient conditions is a high-coverage ambient molecular imaging technique that can map numerous functional metabolites located in different metabolic pathways. Here, we describe the application of AFADESI-MSI metabolomic analysis to define novel diagnostic pathways and metabolites for thyroid follicular tumors, ultimately serving as potential markers of malignant tumors with uncertain potential. Our prospective study aimed to develop and validate an AFAIDESI-MSI metabolomic analysis to define novel diagnostic pathways and metabolites to discriminate between FTA and FTC and improve the diagnosis of indeterminate cases.

## 2. Results

### *2.1. Molecular characterization of thyroid tissues using AFAIDESI-MS imaging and tumor-associated metabolic pathway*

AFAIDESI-MSI was performed in negative and positive ion modes for 24 thyroid tissue samples, including 5 FTC and 19 FTA. Figure 1 shows the MS images of thyroid tumor representative metabolites. We developed a classification model that could distinguish between FTC and FTA samples. Multivariate statistical methods for the training subset included PCA and OPLS-DA. Supervised PCA was initially performed to obtain an overview of all tumors. The differences between the FTA and FTC were explored using OPLS-DA. Threefold cross-validation was performed on a pixel-by-pixel basis in the positive ion mode using the 912 peaks evaluated in the positive mode. Classification of the FTA and FTC groups resulted in one predictive (tB pB) and three orthogonal (tB oB) (1+3) components, with a cross-validated predictive ability, Q 2 (cum) of 73.3%. Additionally, 67.9% of the variance in R 2 (X) accounted for 86.9% of the variance of R 2 (Y), as shown in Supplementary Figure 1A. Among the selected features with the greatest weight for characterizing thyroid tumors were phosphoric acid species, including PC (34:1), PC (36:2), and PC (38:7) (Figure 2A). Negative ion mode data were also analyzed to predict FTC and FTA. Following the same strategy in the negative mode, an overall agreement of 74.2% resulted in one predictive (tB pB) and 13 orthogonal (tB oB) (1+4) components with a cross-validated predictive ability, Q 2 (cum) of 74.2%, and 72.2% of the variance in R 2 (X) accounted for 92.4% of the variance of R 2 (Y) (Supplementary Figure 1B). Among the selected features, several fatty acids (FAs), including FA 20:1 (m/z 309.2038), FA 18:1 (m/z 281.2457), and FA 22:6 (m/z 327.2345) were detected (Figure 2B). Interestingly, all ions exhibited a higher abundance in FTA than in FTC.

Preprints (www.preprints.org) | NOT PEER-REVIEWED | Posted: 15 June 2023 doi:10.20944/preprints202306.1101.v1



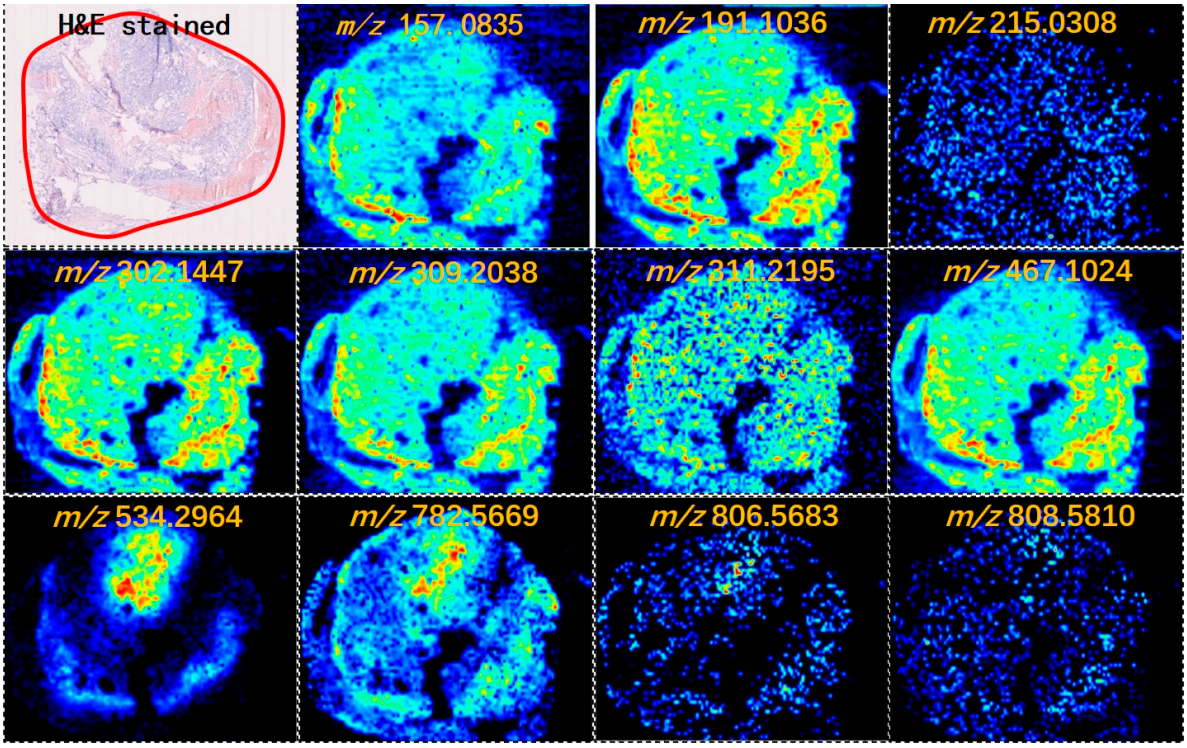


**Figure 1.** The MS images of representative metabolites in thyroid tumor.

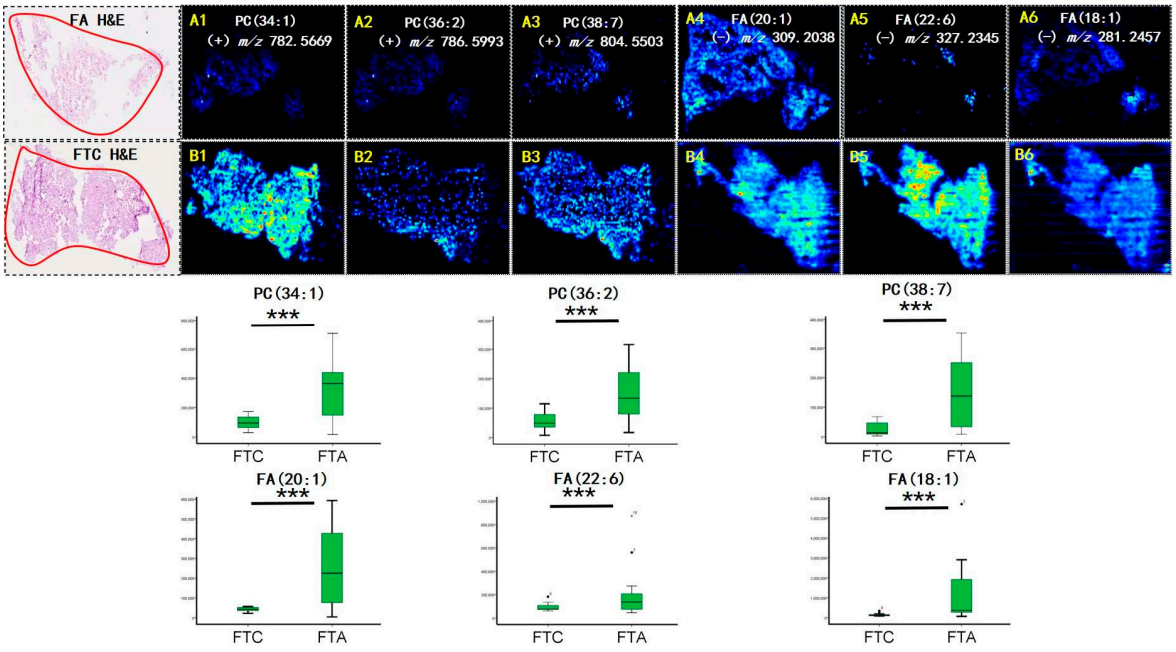


**Figure 2.** AFAIDESI-MSI images of FTA and FTC showing the distribution of (A1, B1) *m/z* 782.5669, PC (34:1); (A2, B2) *m/z* 786.5993, PC(36:2); (A3, B3) *m/z* 804.5503, PC (38:7); (A4, B4) *m/z* 309.2038, FA(20:1); (A5, B5) *m/z* 327.2345, FA(22:6); (A6, B6) *m/z* 281.2457, FA(18:1). The statistical box plots show the ion intensity of metabolites in the lower part. *** $p < 0.001$.

Changes in the expression of metabolic enzymes and related pathways are important characteristics of tumorigenesis. Metabolic enzymes connect and regulate complex metabolic reactions as important nodes in biological metabolic networks and have always been recognized as potential diagnostic markers. Here, AFAIDESI-MSI data combined with OPLS-DA analysis enabled the determination of region-specific metabolites. Subsequently, the discriminating metabolites were imported into the Kyoto Encyclopedia of Genes and Genomes (www.kegg.jp) to perform metabolic pathway

Preprints (www.preprints.org) | NOT PEER-REVIEWED | Posted: 15 June 2023 doi:10.20944/preprints202306.1101.v1



matching analysis, which facilitated the discovery of altered metabolic pathways. This suggests that PC metabolism and FA biosynthesis are significantly dysregulated in thyroid tumors. Notably, two crucial metabolic enzymes were directly associated with alterations in these metabolic enzymes. FASN catalyzed the formation of long-chain FAs, and iPLAs catalyzed the biosynthesis of PC.

*2.2. The protein expression level of FASN and iPLAs were significantly upregulated in thyroid adenoma*

We assessed the classifier's performance identified using IHC staining on an independent set to further evaluate the metabolite enzyme validation. This group included 113 thyroid tumors, including 28 FTC and 66 FTA. The FTC group comprised 6 males and 22 females. Furthermore, the mean age was 47.3 years (ranging: 20–69 years). The FTA group comprised 6 males and 60 females. The mean age was 43.75 years (range: 25–74 years).

Of the 28 FTC, 9 (32.1%) were strongly positive and 19 (67.9%) were weakly-to-moderately positive for FASN. Five (17.9%) iPLAs were strongly positive, 16 (57.1%) were weakly to moderately positive, and 7 (25%) were completely negative for FASN. Of the 66 FTA, 37 (56.1%) were strongly positive for FASN, 28 (42.4%) were weakly to moderately positive, and one (1.5%) was completely negative. Furthermore, 40 (60.6%) iPLAs were strongly positive, 19 (28.8%) were weakly positive, and seven (10.6%) were negative. Interestingly, we noticed that the expression of the metabolic enzyme was significantly higher in the FTA than in the FTC (P=0.043 and P=0.0001 in FASN and iPLAs, respectively) (Table 1). Figure 3 (A,B) shows the metabolic enzyme expression in FTC and FTA.The diagnostic potential of FASN and iPLAs was identified using ROC curve analysis. The AUC, an accuracy index for evaluating the predicting performance, when used for detecting FASN, was 61.4% (95% confidence interval [CI]: 49.2%–73.7%), compared with 71.9% (95% CI: 60.9%–83.0%) for tissue iPLAs. Subsequently, we combined the two biomarkers into a diagnostic combination; ROC curve analysis showed that the AUC was 73.6% (95% CI: 62.7%–84.5%), with a sensitivity and specificity of 82.1% and 60.6%, respectively (Figure 4).

**Table 1.** Performance of the metabolic enzyme expression in FA and FTC.

| Metabolite Enzyme Markers | IHC | Expression Level | FTA(66) | FTC(28) | *p* Value |
|---|---|---|---|---|---|
| FASN | positive | Strong | 37(56.1%) | 9(32.1%) | 0.043 |
| | | Weak-moderated | 28(42.2%) | 19(67.9%) | |
| | Negative | | 1(1.5%) | 0 | |
| IPLAs | positive | Strong | 40(60.6) | 5(17.9%) | 0.0001 |
| | | Weak-moderated | 19(28.8%) | 16(57.1%) | |
| | negative | | 7(10.6%) | 7(25%) | |

Preprints (www.preprints.org) | NOT PEER-REVIEWED | Posted: 15 June 2023 doi:10.20944/preprints202306.1101.v1



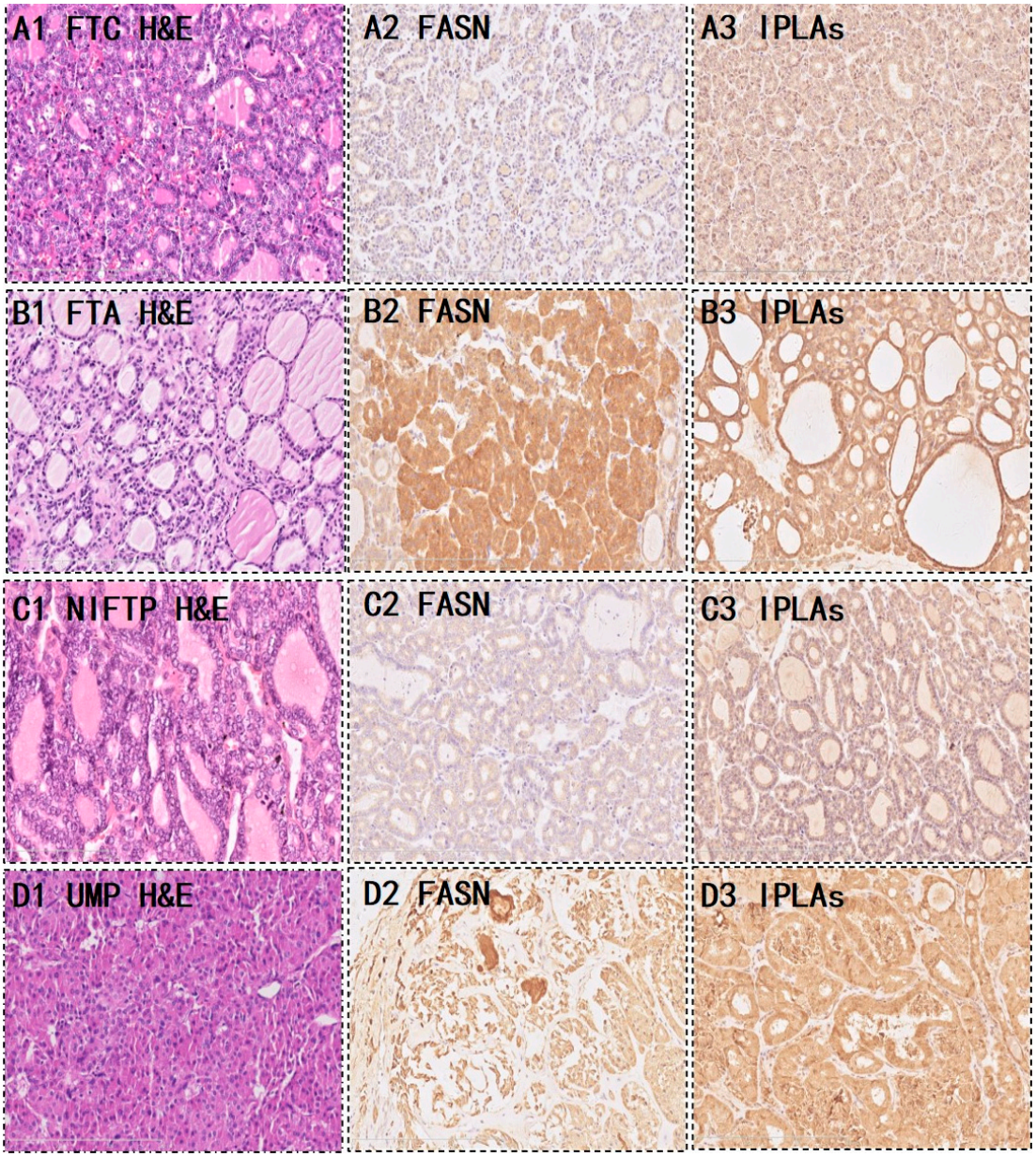


**Figure 3.** Representative microscopic findings for expression of the two metabolic enzymes in FTC(A) and FTA (B), (A1) HE stained for a FTC, (A2) FASN and (A3) IPLAs showed weak or moderate cytoplasmic staining. (B1) HE stained for a FTA, (B2) FASN and (B3) IPLAs showed strong positive staining. (C-D) show the metabolic enzyme expression in borderline thyroid tumors. (C1) and (D1) HE stained for a NIFTP and a UMP, (C2, D2) showed FASN staining and (C3, D3) showed IPLAs staining.

Preprints (www.preprints.org) | NOT PEER-REVIEWED | Posted: 15 June 2023 doi:10.20944/preprints202306.1101.v1



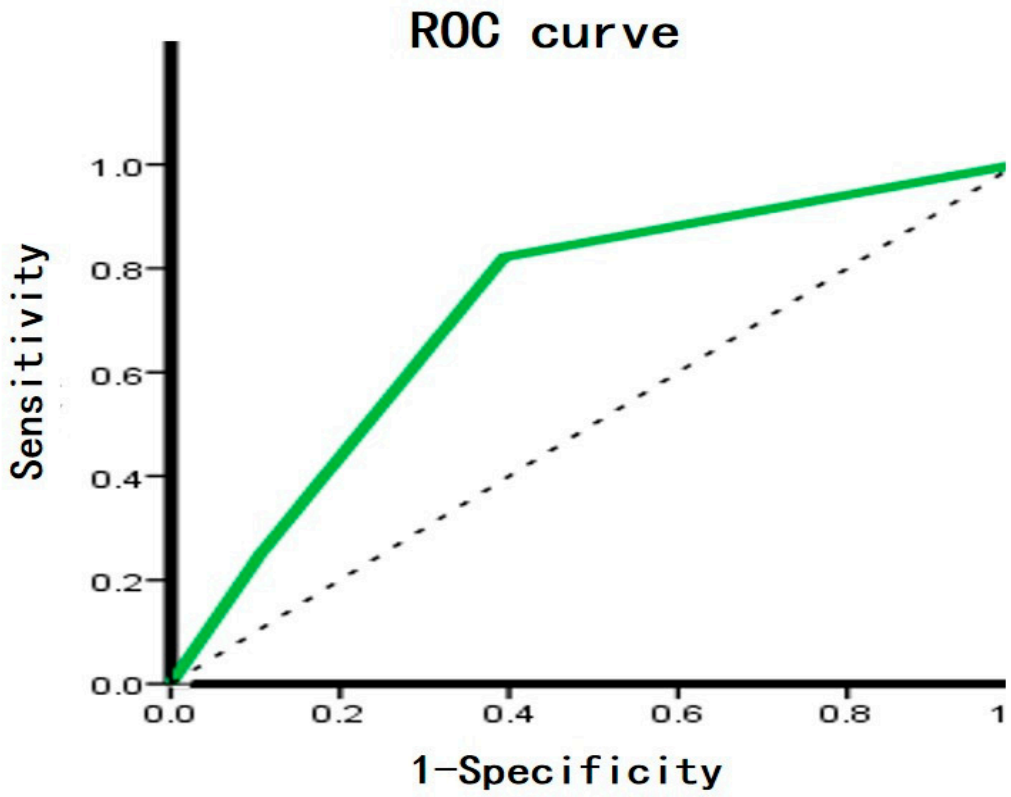


**Figure 4.** ROC analysis of metabolite biomarker between FTA and FTC.

*2.3. Novel diagnostic workflow based on AFAIDESI-MSI analysis and metabolite enzyme markers*

We propose a novel workflow that combines histopathology, AFAIDESI-MSI analysis, and metabolite enzyme markers to diagnose borderline thyroid tumors for implementation in clinical practice. This relies on the performance of the combined metabolic enzyme markers and the predictive model. In the 19 settings, five NIFTP and 14 thyroid tumors of UMP were collected. A significant female predominance was observed in all groups. The female: male ratio was 15:4. The mean age was 42.8 years. The median follow-up was 36.4 (range 11–90) months. From the immunohistochemistry results, 5 (26.3%) cases were more inclined to FTC, and 12 (63.2%) cases were more likely to be FTA (Table 2). Figure 3 (C,D) shows the metabolic enzyme expression in borderline thyroid tumors.

**Table 2.** Predicted diagnosis based on the metabolic enzyme of the 19 nodules with indeterminate thyroid tumors.

| **Histopathology** | **Predicted Diagnosis** | | |
|---|---|---|---|
| | Benign | Gray Zone | Malignant |
| NIFTP(5) | 4 | 0 | 1 |
| UMP(14) | 8 | 2 | 4 |

Two cases could not be classified according to the metabolite enzyme marker results because of inconsistent expression intensities of FASN and iPLAs; therefore, we entered the two cases of mass spectrometry datasets into the predictive model; the results showed that both the two IMS datasets were in the FTA category. Additionally, we randomly selected three borderline cases of MSI data for predictive model analysis; the results of IMS are consistent with the results of metabolite enzyme expression.

 doi:10.20944/preprints202306.1101.v1



## 3. Discussion

Both FTC and FTA are follicular thyroid lesions causing challenging pathological issues. To date, pathologists are virtually unable to draw a clear distinction between FTC and FTA based on a frozen section examination alone. They have some overlapping morphological features; therefore, they represent a diagnostic dilemma for practicing pathologists. A well-known reliable pathological criterion for the malignant diagnosis of FTC is the presence of tumor cells invading the tumor capsule or blood vessels. However, the limited sample collection during the frozen diagnosis process makes evaluating all samples' capsules and blood vessels difficult. Although no envelope or vascular infiltration was found in the paraffin specimen after a comprehensive evaluation, if significant structural and morphological heterogeneity was observed, pathologists could not completely rule out the possibility of malignant tumor biology and could not provide clinically effective diagnosis and treatment guidance.

Therefore, more reliable diagnostic markers are required. To date, there have been an increasing number of markers in the process of continuous evaluation of their diagnostic utility. For example, Kaliszewski et al. [3] proposed that serum thyroid-stimulating hormone levels are significantly higher in patients with atypia and follicular lesions of undetermined significance. Chuang et al. [4] suggested that IHC marker panels, including CK19, CD56, galectin-3, CITED1, HBME-1, VE1, and TROP-2, can differentiate thyroid follicular neoplasms. Nevertheless, none of these biomarkers are used routinely because they lack validity.

AFADESI-MSI is a high-coverage ambient molecular imaging technique that can be used to map numerous functional metabolites in different metabolic pathways. In this study, MSI data combined with OPLS-DA analysis enabled tumor-specific discrimination. For the training set, the score scatter plots for the OPLS-DA models showed very good performance in both the positive and negative ion modes. The expression of phosphoric acid species and FAs was higher in the FA group. MSI-based on *in situ* metabolomics combined with pathway analysis contributed to the discovery of potential tumor-associated metabolic enzymes in thyroid follicular lesions, and targeted IHC testing of the suspected metabolic enzymes—including FASN and iPLAs—was performed on successive tissue sections to validate our discovery. The internal validation of our classification model showed very good performance (95% CI: 62.7%–84.5%, AUC=73.6%, sensitivity=82.1%, specificity= 60.6%).

FAs are essential constituents of all biological membrane lipids and important substrates for energy metabolism. Various tumors and their precursor lesions unexpectedly undergo exacerbated endogenous FA biosynthesis, irrespective of extracellular lipid levels [5–7]. Here, elevated FA levels in the tumor tissue were further confirmed by our MSI results. Figure 1 shows that the FA ion intensities demonstrated an increasing trend from the normal thyroid follicular epithelium to the pathological thyroid tumor epithelia. Interestingly, the ion intensity of FAs in FTA was higher than that in FTC ($P$<0.001, Figure 2C), indicating that FAs may predict potential diagnoses in thyroid follicular tissues. Tumor cells rapidly produce FAs to meet the urgent needs of membrane biosynthesis, cellular signaling, and energy consumption [8]. A multifunctional homodimeric FASN catalyzes the biosynthesis of endogenously synthesized FAs [9–11]. Therefore, FASN is the key metabolic enzyme responsible for the terminal catalytic step in FA synthesis. The subsequent IHC assay showed that FASN was primarily expressed in both FTA and FTC and that its expression was higher in FTA. Some studies have indicated that early upregulation of FASN in precursor lesions might represent an obligatory metabolic acquisition in response to the microenvironment of preinvasive lesions, which continues to occur in malignant stages. The functional and temporal linkage of the glycolytic switch and the FASN-related lipogenic phenotype may represent coevolved essential components of the malignant phenotype and, thus, hallmarks of invasive cancers [12].

Phospholipids are crucial components of the cell membrane. Phosphatidylcholine (PC) is a phospholipid that comprises the majority of cell membranes. De novo biosynthesis of PC occurs via the Kennedy pathway, and perturbations in regulating this pathway have been linked to various human diseases, including cancer [13]. The MS images indicated that phospholipids were significantly upregulated in the FTA tumor region compared to the FTC epithelium (P<0.001, Figure 2C). Over the years, the metabolism of phospholipids by phospholipases and the role of their metabolic products

 doi:10.20944/preprints202306.1101.v1



in mediating cell function have received significant attention. Emerging studies have focused on $Ca^{2+}$-independent PLA2 (iPLA2) enzymes that mediate growth and signaling in numerous cell types. They may offer unique targets for treating various pathologies whose etiology involves the generation of phospholipid signals [14]. Some studies have demonstrated that iPLA2 mediates cell growth by participating in signal transduction pathways, including epidermal growth factor receptors, mitogen-activated protein kinases, mdm2, tumor suppressor protein p53, and cell cycle regulator p21 [15–19]. We speculate that the upregulated expression of iPLA2 in thyroid follicular tumors may be attributed to elevated phospholipid biosynthesis. IHC staining was performed to explore the spatial expression of iPLA2 in the thyroid follicular tumor sections. Similarly, IHC analysis indicated that iPLA2 expression was significantly higher in FTA.

Subsequently, we focused on 19 indeterminate pathological diagnoses; a prediction of non-malignancy was obtained in 12 of the 19 patients that agreed with the follow-up, and 5 with a suspicious diagnosis were malignant. Due to the inconsistent expression intensity of FASN and iPLAs, two cases could not be classified according to the metabolite enzyme marker results; the two cases of mass spectrometry dataset predictive results were in the category of FTA. There are some explanations for this inconsistent expression as follows: the distribution of diagnostic cells in the sample can be heterogeneous, presenting sparse and/or overlapping cellular content, which the instability of IHC antibodies may also cause. Therefore, this implementation of combined AFAIDESI-MSI with metabolite enzyme markers positively affects diagnosis classification for the “indeterminate” nodules.

## 4. Materials and Methods

### *4.1. Sample collection*

All thyroid tumor tissue samples were collected at the Peking Union Medical College Hospital between 2014 and 2021. The Ethical Review Committee of the Peking Union Medical College Hospital approved the study protocols. All patients consented to participate in this study and signed an informed consent form. All experiments were performed in accordance with the approved guidelines. Notably, none of the patients with thyroid cancer underwent preoperative treatment. The tumor tissue samples obtained from surgical resection specimens were snap-frozen and stored at -80°C until sectioning. For the AFAIDESI-MSI experiments, 8-μm-thick tissue sections were cut at -20°C using a cryomicrotome (CM 1950; Leica, Wetzler, Germany) and thaw-mounted onto microscope glass slides (Superfrost Plus slides, Thermo Fisher Scientific, USA). The slides were stored in closed containers at -80°C. Before the analysis, the slides were thawed at room temperature and dried in a vacuum desiccator for approximately 1 h. Five-micrometer-thick tissue sections were cut and stained with hematoxylin and eosin (H&E) to confirm the diagnosis.

MSI was performed using a Q Orbitrap mass spectrometer (Q Exactive, Thermo Fisher Scientific, Waltham, MA, USA) equipped with a home-built AFADESI ion source. Data were acquired in both positive and negative ion modes. The measurement conditions were as follows: the ESI sprayer was positioned 0.7 mm away from the tissue surface at an incident angle of 55° to the sample surface. The spray solvent for MS acquisition in the positive mode was acetonitrile: water (8:2, *v*/*v*) containing 0.1% formic acid with a (±) 7000 V spray voltage, and the transport tube voltage (±) 3000 V. Acetonitrile (ultra-pure water) was purchased from Germany. The solvent and extraction flow rates were 5 and 45 L/min, respectively. In the tissue imaging experiments, each tissue section was scanned using a two-dimensional (2D) moving stage with horizontal rows separated by a 200-μ m vertical step until the entire tissue sample was assayed. All experiments were conducted using Analyst QS 2.0. Mass spectra were recorded in the mass range of m/z 100–1000.

### *4.3. Histopathology analysis*

All specimens were fixed in 10% buffered neutral formalin and embedded in paraffin. Tumor content was determined by examining H&E-stained tissue sections adjacent to the sections used for the AFAIDESI-MSI studies. The slides were re-evaluated histologically and classified according to the 2022 WHO criteria. Two pathologists determined tumor content by examining H&E-stained

tissue sections adjacent to the sections used for the AFAIDESI-MSI studies. The tissue slides were free of necrosis.

*4.4. Immunohistological stains*

The expression of metabolic enzymes in thyroid tumor tissues was assessed by immunohistochemical (IHC) staining using specific antibodies. Successive frozen tissue sections adjacent to the section analyzed using AFADESI-MSI were warmed to room temperature for 20 min. Sections were fixed in paraformaldehyde for 10 min. After washing in phosphate-buffered saline, the sections were immersed in 0.25% Triton X-100 for 15 min to make the tissue permeable and then blocked with 1% bovine serum albumin for 30 min at room temperature. Furthermore, the sections were incubated with antibodies against iPLAs (Proteintech; 22030-1-AP; 1:200), fatty acid synthase (FASN) (Abcam; ab128870;1:300) at 4°C overnight, followed by rewarming at room temperature for 20 min. A PV-9000 two-step IHC kit was used according to the manufacturer's instructions, and a DAB kit was used to detect antigen-antibody binding (Zhongshan Goldenbridge Biotechnology Ltd. Co., Beijing, China). The slides were counterstained with hematoxylin, dehydrated, mounted, and covered. FASN and iPLAs staining revealed cytoplasmic protein expression. The intensities of FASN and iPLAs were graded semi-quantitatively on a scale of 0 (no staining), low expression (weak staining), and high expression (moderate to strong staining).

*4.5. Data processing and statistical analysis*

All tissue samples were subjected to AFAIDESI-MSI. Raw data files acquired from the AFAIDESI-MS analysis were initially converted to MATLAB format using the Wiff-to-Matlab translator software. A software tool was developed to enable visual inspection of the ion image and selection of regions of interest (ROIs). ROIs were selected using H&E staining, and the corresponding spectral data were extracted from each ROI. The resultant 2D matrices, including observations (sample names) in columns and variables (m/z) in rows, were subsequently transferred to MarkerView (Applied Biosystems/MDS Sciex) and SIMCA version 14.0.1 software package (Umetrics AB, Umeå, Sweden). Pareto scaling and normalization with ion intensity were applied to all data to reduce noise and artifacts in the models. Moreover, the multivariate statistical methods used included principal component analysis (PCA) and orthogonal partial least square discriminant analysis (OPLS-DA). After classification, discriminating variables were selected according to variable importance and assessed using an independent *t*-test (Microsoft Office Excel 2010). Statistical significance was set at $P<0.05$. Moreover, accurate mass spectrometry and MS/MS analyses were performed using a Q-Orbitrap mass spectrometer (Q-Exactive, Thermo Fisher Scientific) for molecular identification. Lipid species were first analyzed by comparing the mass measurement of each peak with that in the LIPID MAPS database (http://lipidmaps.org; mass accuracy ± 0.005 Da) and then identified based on collision-induced dissociation experiments, tandem MS experiments, and comparison with data from the literature. A receiver operating characteristic (ROC) curve analysis was performed to determine the roles of accuracy and specificity in the predictability of certain indicators. The area under the curve (AUC) ranged from 0.5 to 1.0. Complete separation of the values by indicator was performed with scores above 0.75 or 75%.

## 5. Conclusions

We show evidence that the combination of AFAIDESI-MSI and metabolite enzyme markers is a promising approach to aid the diagnosis of thyroid follicular nodules. Particularly in cases of "gray zone category" follicular tumors, lower FASN and iPLAs combined with a diagnosis of thyroid follicular borderline tumor should be considered for strict follow-up.

**Supplementary Materials:** The following supporting information can be downloaded at the website of this paper posted on Preprints.org. Supplementary Materials: Figure S1A: OPLS-DA score plots based on positive AFAIDESI-MSI data from FTC and FTA; Figure S1B: OPLS-DA score plots based on negative AFAI-MSI data from FTC and FTA; Table S1: The discriminated meatbolites between FTA and FTC.

**Author Contributions:** Conceptualization, J.C. and J.H.; methodology, T.L.; software, T.L.; validation, X.M., formal analysis, L.H.; investigation, L.H. and X.M.; resources, X.M.; data curation, L.H.; writing—original draft preparation, X.M.; writing—review and editing, J.C.; visualization, X.M.; supervision, J.C. and J.H.; project administration, Z.A.; funding acquisition, J.H. and J.C. All authors have read and agreed to the published version of the manuscript.

**Funding:** This research was funded by the National High Level Hospital Clinical Research Funding, grant number 2022-PUMCH-A-027.

**Institutional Review Board Statement:** The study was conducted in accordance with the Declaration of Helsinki, and approved by the Ethics Committee of Peking Union Medical College Hospital (protocal code JS-2557).

**Informed Consent Statement:** Informed consent was obtained from all subjects involved in the study.

**Data Availability Statement:** The data presented in this study are contained within the article and Supplementary Materials.

**Conflicts of Interest:** The authors declare no conflict of interest.

**Sample Availability:** Samples of the metabolites standard substances are available from the authors.

## References

1. Siegel, R.L.; Miller K.D.; Jemal A. Cancer statistics, 2019. *CA. Cance.r J. Clin.* **2019**, *69*, 7-34.
2. Goodarzi, E.; Moslem, A.; Feizhadad, H.; Jarrahi, A.; Adineh, H.; Sohrabivafa, M.; et al. Epidemiology, incidence and mortality of thyroid cancer and their relationship with the human development index in the world: an ecology study in 2018. *Adv. Hum. Biol.* **2019**, *9*, 162-167; DOI:10.4103/AIHB.AIHB_2_19.
3. Kaliszewski, K.; Diakowska, D.; Rzeszutko, M.; Nowak, Ł.; Wojtczak, B.; Sutkowski, K.; et al. Assessment of preoperative TSH Serum level and thyroid cancer occurrence in patients with AUS/FLUS thyroid nodule diagnosis. *Biomedicines.* **2022**, *10*, 1916; DOI:10.3390/biomedicines10081916.
4. Chuang, H.W.; Wang, J.S.; Tsai, J.W.; Hsu, C.T.; Lin, K.J. Immunohistochemistry helps to distinguish noninvasive follicular thyroid neoplasm with papillary-like nuclear features/noninvasive encapsulated follicular variant of papillary thyroid carcinoma with other follicular thyroid lesions. *Medicina (Kaunas).* **2021**, *57*, 1246; DOI:10.3390/medicina57111246.
5. Swinnen, J.V.; Brusselmans, K.; Verhoeven, G. Increased lipogenesis in cancer cells: new players, novel targets. *Curr. Opin. Clin. Nutr. Metab. Care.* **2006**, *9*, 358-365; DOI:10.1097/01.mco.0000232894.28674.30.
6. Menendez, J.A.; Lupu, R. Oncogenic properties of the endogenous fatty acid metabolism: molecular pathology of fatty acid synthase in cancer cells. *Curr. Opin. Clin. Nutr. Metab. Care.* **2006**, *9*, 346-357; DOI:10.1097/01.mco.0000232893.21050.15.
7. Kuhajda, F.P. Fatty acid synthase and cancer: new application of an old pathway. *Cancer. Res.* **2006**, 66, 5977-5980; DOI:10.1158/0008-5472.CAN-05-4673.
8. Kuhajda, F.P. Fatty-acid synthase and human cancer: new perspectives on its role in tumor biology. *Nutrition.* (**2000**) *16,* 202-208; DOI: 10.1016/s0899-9007(99)00266-x.
9. Chirala, S.S.; Wakil, S.J. Structure and function of animal fatty acid synthase. *Lipids.* **2004**, *39*, 1045-1053; DOI:10.1007/s11745-004-1329-9.
10. Asturias, F.J.; Chadick, J.Z.; Cheung, I.K.; Stark, H.; Witkowski, A.; Joshi, A.K.; et al. Structure and molecular organization of mammalian fatty acid synthase. *Nature. Struct. Mol. Biol.* ***2005***, *12*, 225-232; DOI:10.1038/nsmb899.
11. Maier, T.; Jenni, S.; Ban, N. Architecture of mammalian fatty acid synthase at 4.5 Å resolution. *Science.* ***2006***, *311*, 1258-1262; DOI:10.1126/science.1123248.
12. Menendez, J.A.; Lupu, R. Fatty acid synthase and the lipogenic phenotype in cancer pathogenesis. *Nat. Rev. Cancer.* **2007**, *7,* 763-777; DOI:10.1038/nrc2222.
13. Stoica, C.; Ferreira, A.K.; Hannan, K.; Bakovic, M. Bilayer forming phospholipids as targets for cancer therapy. *Int. J. Mol. Sci.* **2022**, *23*, 5266; DOI:10.3390/ijms23095266.
14. Zhang, X.H.; Zhao, C.; Ma, Z.A. The increase of cell-membranous phosphatidylcholines containing polyunsaturated fatty acid residues induces phosphorylation of p53 through activation of ATR. *J. Cell. Sci.* **2007**, *120*, 4134-4143; DOI:10.1242/jcs.015834.

15. Sun, B.; Zhang, X.; Talathi, S.; Cummings, B.S. Inhibition of Ca2+-independent phospholipase A2 decreases prostate cancer cell growth by p53-dependent and -independent mechanisms. *J. Pharmacol. Exp. Ther.* **2008**, *326*, 59-69; DOI:10.1124/jpet.108.138958.
16. Song, Y.; Wilkins, P.; Hu, W.; Murthy, K.S.; Chen, J.; Lee, Z.; et al. Inhibition of calcium-independent phospholipase A2 suppresses proliferation and tumorigenicity of ovarian carcinoma cells. *Biochem. J.* **2007**, *406*, 427-436; DOI:10.1042/BJ20070631.
17. Zhang, X.H.; Zhao, C.; Seleznev, K.; Song, K.; Manfredi, J.J.; Ma, Z.A. Disruption of G1-phase phospholipid turnover by inhibition of Ca2+-independent phospholipase A2 induces a p53-dependent cell-cycle arrest in G1 phase. *J. Cell. Sci.* **2006**, *119*, 1005-1015; DOI:10.1242/jcs.02821.
18. Korbecki, J.; Bosiacki, M.; Gutowska, I.; Chlubek, D.; Baranowska-Bosiacka, I. Biosynthesis and Significance of Fatty Acids, Glycerophospholipids, and Triacylglycerol in the Processes of Glioblastoma Tumorigenesis. *Cancers*. **2023**, *15*, 2183; DOI:10.3390/cancers15072183.
19. Lei, X.; Zhang, S.; Bohrer, A.; Bao, S.; Song, H.; Ramanadham, S. The group VIA calcium-independent phospholipase A2 participates in ER stress-induced INS-1 insulinoma cell apoptosis by promoting ceramide generation via hydrolysis of sphingomyelins by neutral sphingomyelinase. *Biochemistry.* **2007**, *46*, 10170-10185; DOI:10.1021/bi700017z.